Available online at www.sciencedirect.com
ScienceDirect
Ceramics International 38 (2012) 487–493
CERAMICS INTERNATIONAL
www.elsevier.com/locate/ceramint

In situ preparation of SiC/Si_3N_4-NW composite powders by combustion synthesis

Chao-Sheng Zheng [a], Qing-Zhi Yan [a,*], Min Xia [b], Chang-Chun Ge [a]

[a] *Laboratory of Special Ceramics and Powder Metallurgy, University of Science and Technology Beijing, Beijing 100083, People's Republic of China*
[b] *Institute of Powder Metallurgy and Advanced Ceramics, Southwest Jiaotong University, Chengdu 610031, People's Republic of China*

Received 3 May 2011; received in revised form 10 July 2011; accepted 18 July 2011
Available online 26th July 2011

Abstract

Large-scale composite powders containing silicon carbide (SiC) particles and silicon nitride nanowires (Si_3N_4-NWs) were synthesized in situ by combustion synthesis (CS). In this process, a mixture of silicon, carbon black, polytetrafluoroethylene (PTFE) and a small amount of iron powders was used as the precursor. The products were characterized by XRD, SEM, EDS and TEM. The particles are equiaxed with diameters in the micron range, and the in situ formed nanowires are straight with uniform diameters of 20–350 nm and lengths of tens of microns. The Si_3N_4-NWs are characterized to be α-phase single crystals grown along the [1 0 1] or [1 0 0] direction. VLS and SLGS processes are proposed as the growth mechanisms of the nanowires. The as-synthesized powders have great potential for use in the preparation of high-performance SiC/Si_3N_4-NW composites.

Keywords: D. SiC; D. Si_3N_4; Combustion synthesis; Nanowires

1. Introduction

Due to high hardness, excellent oxidation, corrosion and wear resistance, and high temperature mechanical properties such as strength retention and creep resistance, silicon carbide (SiC) is one of the promising ceramic materials for use as structural components in heat engines and high-temperature conversion systems such as turbines. For the use of SiC in such applications fracture toughness of the material is a critical consideration. However, commercial SiC ceramics have relatively low fracture toughness, in the order of about 3–5 MPa $m^{1/2}$. Prior investigations have demonstrated that the fracture toughness of ceramics can be improved significantly through reinforcement with high-strength whiskers [1–6], or fibers [7,8].

One-dimensional nanostructures, such as nanotubes and nanowires, have great potential for use as reinforcements in composites because they exhibited superior properties compared with their bulk counterparts [9–12]. Recently, Si_3N_4-NWs have attracted intense interest due to their excellent properties, such as wide band gap, high strength, high hardness, and good resistance to thermal shock and oxidation. Several routes have been developed for the synthesis of Si_3N_4-NWs, such as chemical vapour deposition [13], carbothermal reduction [14–16], nitridation of Si or SiO powder [17,18], carbon-nanotube-confined chemical reaction [19]. However, when pre-formed nanowires are employed to reinforce ceramic materials, it has been very difficult to homogeneously mix the nanowires with matrix powder due to their initial agglomerated state. The mass of agglomerated nanowires when used as reinforcement will produce a non-homogeneous composite of lower mechanical strength. One way to overcome the above difficulty is to process composite ceramic powders containing in situ-formed nanowires.

The combustion synthesis (CS), or self-propagating high temperature synthesis (SHS) is based on the fact that the strong exothermic reaction, which occurs during the formation of the compound, can propagate rapidly through the solid reactants. CS has evident advantages: low energy requirement, high product purity, simple and cheap equipment, high sinterability of product, and possible nonequilibrium phases in the products [20]. While the CS is widely used to prepare SiC and Si_3N_4

* Corresponding author. Tel.: +86 010 6233 4951; fax: +86 010 6233 4951.
E-mail address: qingzhiyan111@163.com (Q.-Z. Yan).

0272-8842/$36.00
doi:10.1016/j.ceramint.2011.07.032

powders [20–26], there have been much less reports focused on the CS of Si_3N_4 whiskers/fibers. Rodriguez et al. [27] reported CS of β-Si_3N_4 fibers via silicon nitridation under 10 MPa nitrogen pressure. α-Si_3N_4 whiskers were successfully synthesized by Cao et al. [28] through CS under 1 MPa N_2 with addition of NaN_3 as catalyst.

In this study, large-scale composite powders containing SiC particles and Si_3N_4-NWs were prepared by cost effective CS under 2 MPa N_2, using the mixture of Si, carbon black, PTFE and a small amount of iron powders as the precursor. These nanowires were in situ formed and homogeneously dispersed among the SiC particles. Thus the composite powders have great potential for use in the preparation of high-performance ceramic composites.

2. Experimental procedure

In this study, elemental Si (1–3 μm, 99% pure), carbon black (24 nm, 99% pure) and PTFE (99% pure) powders were used as raw materials. The starting materials had a mixing ratio of PTFE: (Si + C) = 15:100 (wt) and Si:C = 1:1 (mol). A small amount of Fe powders (3 μm) were also introduced as the catalyst. The mixture was thoroughly ball milled in ethanol for 10 h and then dried in air. The resulting powders were packed directly into a porous graphite crucible. The combustion experiments were preformed in a high pressure combustion vessel (60 L in volume) under 2 MPa nitrogen pressure. The combustion was initiated by burning the titanium powder placed on the top of the reactant using a tungsten coil. The temperature–time curve was measured by a W-5%Re/W-26%Re thermocouple of ∅0.5 mm, whose tip was embedded in the powder near the surface. The experiments were also performed on the samples without Fe additives for comparison. In each batch, several hundred grams of product could be obtained. The combustion products were characterized by X-ray diffraction (XRD). The morphologies were analyzed by a field-emission scanning electron microscope (FESEM). The transmission electron microscope (TEM) was used to characterize the microstructures of the products.

3. Results and discussion

Two-group experiments were carried out for comparison. The product of Fe-assist experiment was labeled as product A and the product of catalyst-free experiment as product B. The product A was found to be gray viscous powders. After the product A being treated in air at 650 °C for 1 h, the powders turned yellow-green, indicating that there was quite a lot of elemental carbon in the primary product. On the other hand, the product B was yellow-green free flowing powders.

3.1. Morphologies of the combustion products

The morphologies of as-obtained powders were studied by FESEM and TEM firstly (Figs. 1 and 2). Fig. 1 is the FESEM images of the product A at different magnifications, showing that a number of nanowires randomly distribute among the particles. Most of the nanowires are straight with uniform diameters of 20–350 nm and lengths of up to tens of microns. The particles are equiaxed with diameters in the micron range, and several to tens of particles were usually sintered together to form a larger one. Besides, no nanowires were observed in the product B, which reveals that iron powders played a key role in the formation of the nanowires. TEM was also used to further characterize the morphology of the nanowires (shown in Fig. 2). It can be clearly seen from Fig. 2 that the as-produced nanowires have smooth surface with similar dimensions to those observed by FESEM. The nanowires are almost transparent, for the lower nanowire can be seen through the upper one at the intersection.

3.2. Crystallography and chemical compositions

The crystalline structures of the combustion products were first examined using XRD (CuKα) (shown in Fig. 3). The patterns show that the product A predominantly consists of 3C-SiC and α-Si_3N_4 while the product B is pure cubic SiC. The unit cell refinement gave the cell parameters $a = 4.364$ Å for 3C-SiC and $a = 7.766$ Å, $c = 5.596$ Å for α-Si_3N_4, which are close to the reported value for 3C-SiC ($a = 4.359$ Å, PDF Card. No. 29-1129) and α-Si_3N_4 ($a = 7.758$ Å, $c = 5.623$ Å, PDF Card.

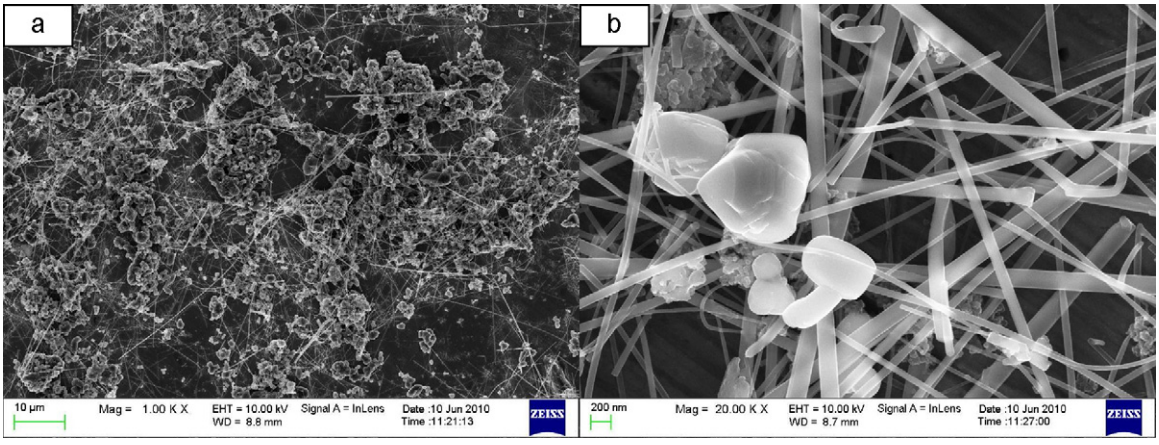

Fig. 1. FESEM images of the product A (Fe as the catalyst) at different magnifications.

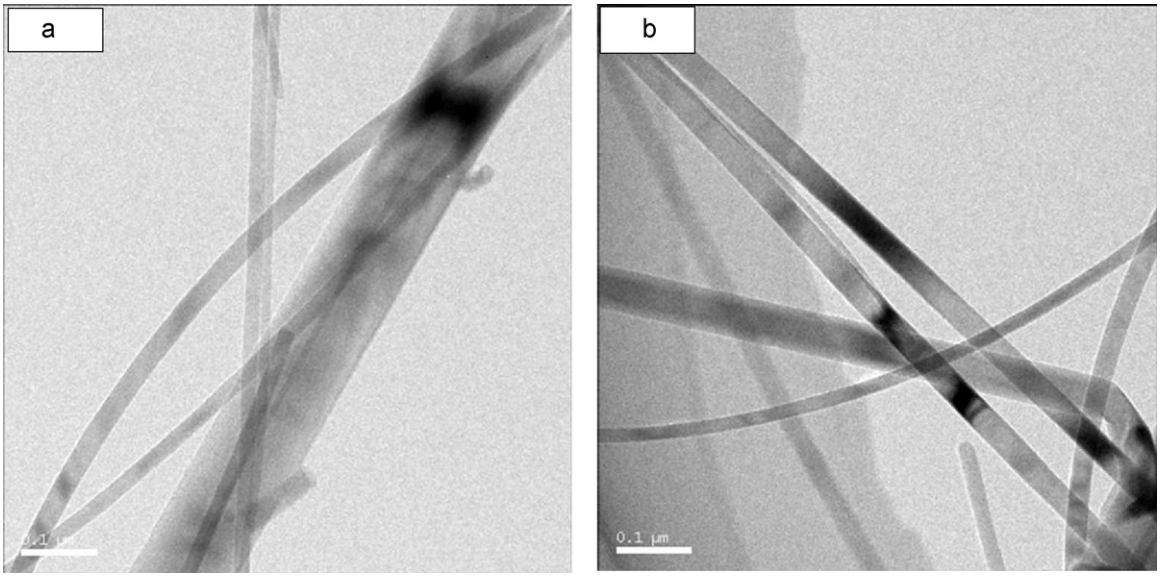

Fig. 2. TEM images of the nanaowires from the product A (Fe as the catalyst).

No. 09-0250) respectively. Clearly, the intensities of the α-Si_3N_4 peaks are much lower than that of the 3C-SiC peaks. The peak near $2\theta = 45.2^\circ$ (labeled with ◇) indicates that the catalyst of Fe is being in the form of Fe_3Si in the product A. The XRD patterns reveal that iron powders promoted the formation of α-Si_3N_4 crystals during combustion process. Fig. 4 depicts the typical EDS images of an individual particle and nanowire from the product A. The images show that the particles consist of the elements Si and C (Fig. 4(a)) and the nanowires consist of elements Si and N (Fig. 4(b)). The Cu peaks are from the copper plate on which the powders were loaded, and the peak near 2.15 keV can be assigned to Au, which was introduced during the specimen preparation. Hence, we can get a conclusion that the particles are 3C-SiC and the nanowires are α-Si_3N_4. This can explain why the product A contains a lot of free carbon. It is simply because quite an amount of element Si has been transformed to Si_3N_4 instead of SiC when the raw material had a mixing ratio of Si:C = 1:1 (mol). There are two main reasons why α-Si_3N_4 exhibits such low intensity peaks relative to 3C-SiC in the XRD pattern of the product A. Firstly, materials with cubic structure (3C-SiC) have stronger diffraction intensities compared to hexagonal structures (α-Si_3N_4). In quantitative analysis, this is incorporated to the $K_{j(h\ k\ l)}$, what is a constant for the reflection (*h k l*) plane [29]. Secondly, the Si_3N_4-NWs have much smaller diameters (most below 100 nm) and preferred orientations compared to the SiC particles.

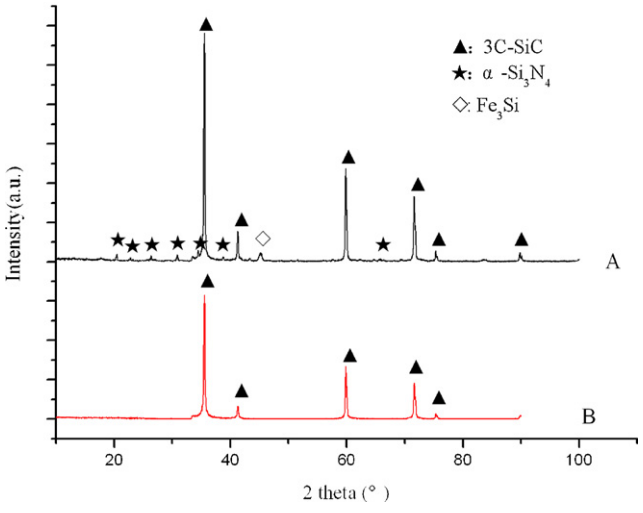

Fig. 3. XRD patterns of the combustion products (A and B).

Further characterization of the crystalline structures of the nanowires was operated using SAED and HRTEM (Fig. 5). Panels of Fig. 5(b) and (d) are corresponding HRTEM lattice images of the nanowires shown in Fig. 5(a) and (c) respectively. SAED patterns obtained from the [0 1 0] (inset in Fig. 5(a)) and [0 0 1] (inset in Fig. 5(c)) zone axes confirm that the nanowires are single crystals of α-Si_3N_4. HRTEM images reveal that the nanowires possess a perfect crystal structure with few structure defects such as dislocations and stacking faults. The measured *d* spacings of 0.672, 0.562, 0.433 and 0.386 nm are in good agreement with (1 0 0), (0 0 1), (1 0 1) and (1 1 0) planes of bulk α-Si_3N_4 ($a = 7.758$ Å, $c = 5.623$ Å, PDF Card. No. 09-0250). Both SAED patterns and HRTEM images suggest that [1 0 1] (Fig. 5(a) and (b)) and [1 0 0] (Fig. 5(c) and (d)) are growth directions for the α-Si_3N_4 nanowires. Besides, the surface of the nanowire shown in Fig. 5(a) and (b) possesses a thin amorphous layer, which is amorphous SiO_x, while the other nanowire shown in Fig. 5(c) and (d) has a clear surface.

3.3. Growth mechanisms

The combustion synthesis is involved with abrupt release of large amount of heat resulting in high temperature. Fig. 6 depicts the variation of temperature with time during combustion synthesis under 2 MPa nitrogen pressure. The

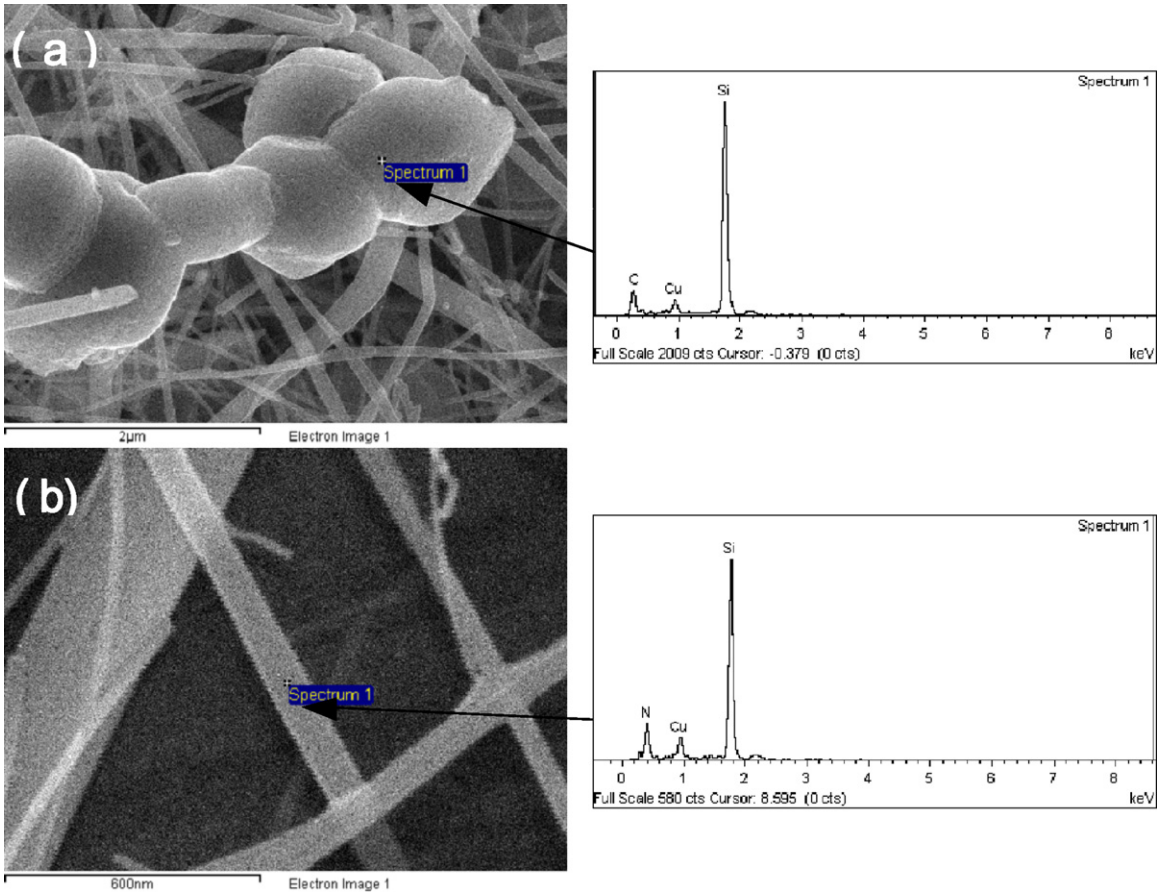

Fig. 4. (a) Typical EDS image of the individual particle from the product A. (b) Typical EDS image of the individual nanowire from the product A.

combustion temperature increased abruptly to 1120 °C (T_1) within 1 s, which was ascribed to the nitridation of Si occurred from the particle surface [21]. After several seconds, the temperature dropped suddenly to 960 °C and then increased to 1337 °C (T_2) due to the reaction of silicon and PTFE which will be mentioned later. T_2 is the highest temperature during the combustion process. However, Si_3N_4 was thermodynamically more stable than SiC in this temperature range under 2 MPa N_2 [30]. From the mechanism reported by Yamada et al. [21], SiC was formed via the reaction of silicon and carbon in a nonequilibrium process due to the difference in vapour pressure of Si for Si_3N_4 and SiC at experimental temperatures. In addition, we suppose the nanowires should be formed after the nitridation of silicon particles.

Several models including VLS (vapour–liquid–solid) [31], VS (vapour–solid) [18], OAG (oxide-assisted growth) [32], and SLS (solution–liquid–solid) [33] mechanisms have been proposed to explain the growth of 1-D structures. In our work, the catalyst of Fe played a key role in the growth of α-Si_3N_4 nanowires, and catalyst-assist growth of whiskers has been widely explained by the VLS mechanism [14,15,31]. The main feature of the VLS mechanism is the existence of intermediates that act as the energetically favored site for absorption of gas-phase reactant, and the morphology feature is a catalyst droplet on the tip of the whisker. As shown in Fig. 7(a), the as-synthesized nanowires include some wires with a ball on the tip. Chemical analysis reveals that the ball should be a catalyst droplet with the chemical composition of Fe, Si and C elements, and the nanowire only consists of Si and N elements. Hence, such nanowires were formed by the VLS mechanism. Firstly, Fe particles reacted with Si and C particles to form liquid Fe–Si–C alloy at a temperature higher than the eutectic temperature of Fe–Si–C ternary system. The Si atoms in the liquid alloy reacted with N_2 gas in the liquid/gas interface to form Si_3N_4 embryos. When the embryos grew large enough, a small amount of liquid alloy was lifted by the crystal, producing a catalyst droplet. Then, the silicon atoms for the nanowire growth were only supplied through vapour-phase migrations (silicon vapour, SiO, and SiF_4) instead of liquid-phase diffusion. The O element may come from the N_2 atmosphere and silicon oxides due to partial oxidation of silicon particles before combustion, and that some nanowires posses SiO_x layer (Fig. 5(a) and (b)) may relate to this growth process. The origin of SiF_4 will be mentioned later.

After careful examination, however, we find that most of the as-synthesized nanowires have no catalyst droplets on their tips, which indicates that another growth mechanism should be responsible for the growth of most nanowires. Recently, Yang et al. [34,35] proposed a unique SLGS (solid–liquid–gas–solid) mechanism to explain the growth of α-Si_3N_4 nanobelts and nanowires, which were synthesized by thermal decomposition of a polysilazane preceramic polymer using $FeCl_2$ as catalyst.

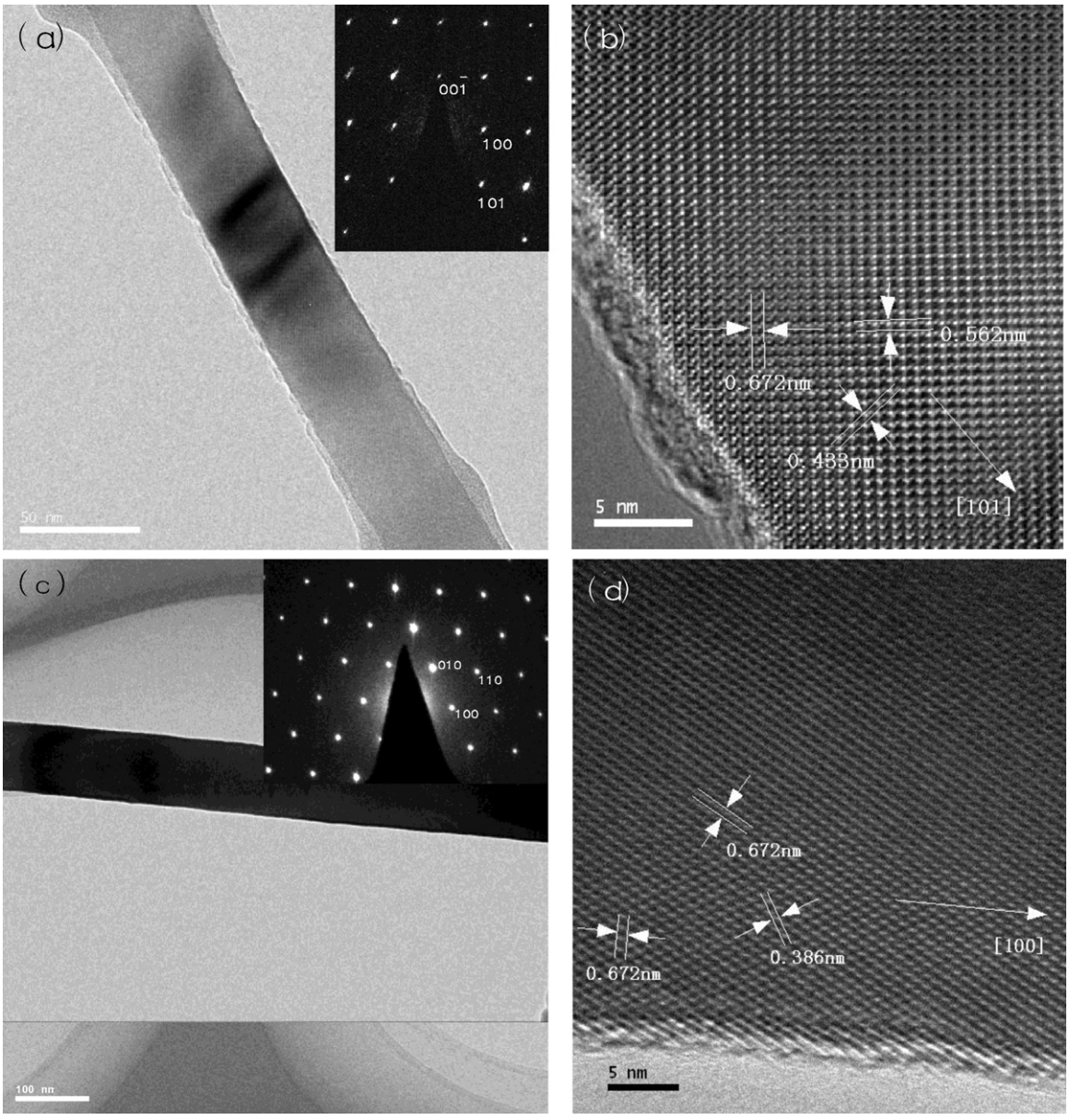

Fig. 5. (a) TEM image with corresponding SAED pattern (inset) of one Si_3N_4-NW grown along [1 0 1] direction. (b) The corresponding HRTEM lattice image of the nanowire shown in (a). (c) TEM image with corresponding SAED pattern (inset) of one Si_3N_4-NW grown along [1 0 0] direction. (d) The corresponding HRTEM lattice image of the nanowire shown in (c).

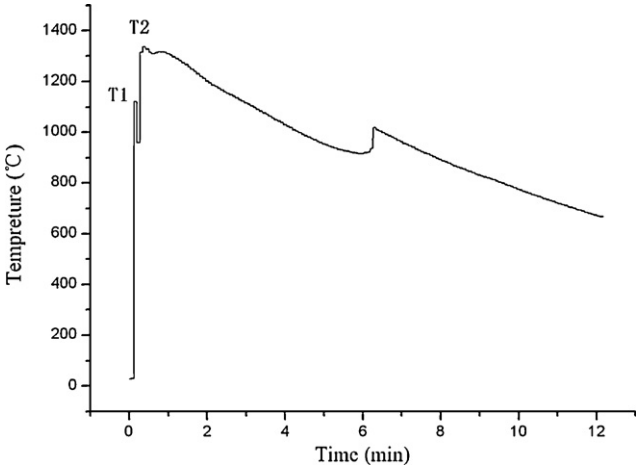

Fig. 6. Temperature histories of the combustion synthesis.

The SLGS mechanism could well explained the growth of the nanowires without catalyst droplets in present work. In the process of combustion, Fe particles firstly reacted with Si and C particles and liquid Fe–Si–C alloy was formed. Further reaction of these elements made the liquid alloy supersaturated with Si and C. The supersaturated liquid reacted with N_2 in the liquid/gas interface, thus resulting in the precipitation of Si_3N_4-NWs due to the size confining effect of the liquid phase. In this process, Si atoms for the nanowire growth were supplied through liquid-phase diffusion. From Fig. 7(b) we can see that several nanorods have grown from the points (labeled with black arrow) between crystalline grains, and Fig. 7(c) clearly depicts that one nanowire has grown from the interspace among several particles. In the process of combustion, the liquid alloy flowed in the interspace between neighboring particles and the nanowires grew from the liquid phase via the SLGS process.

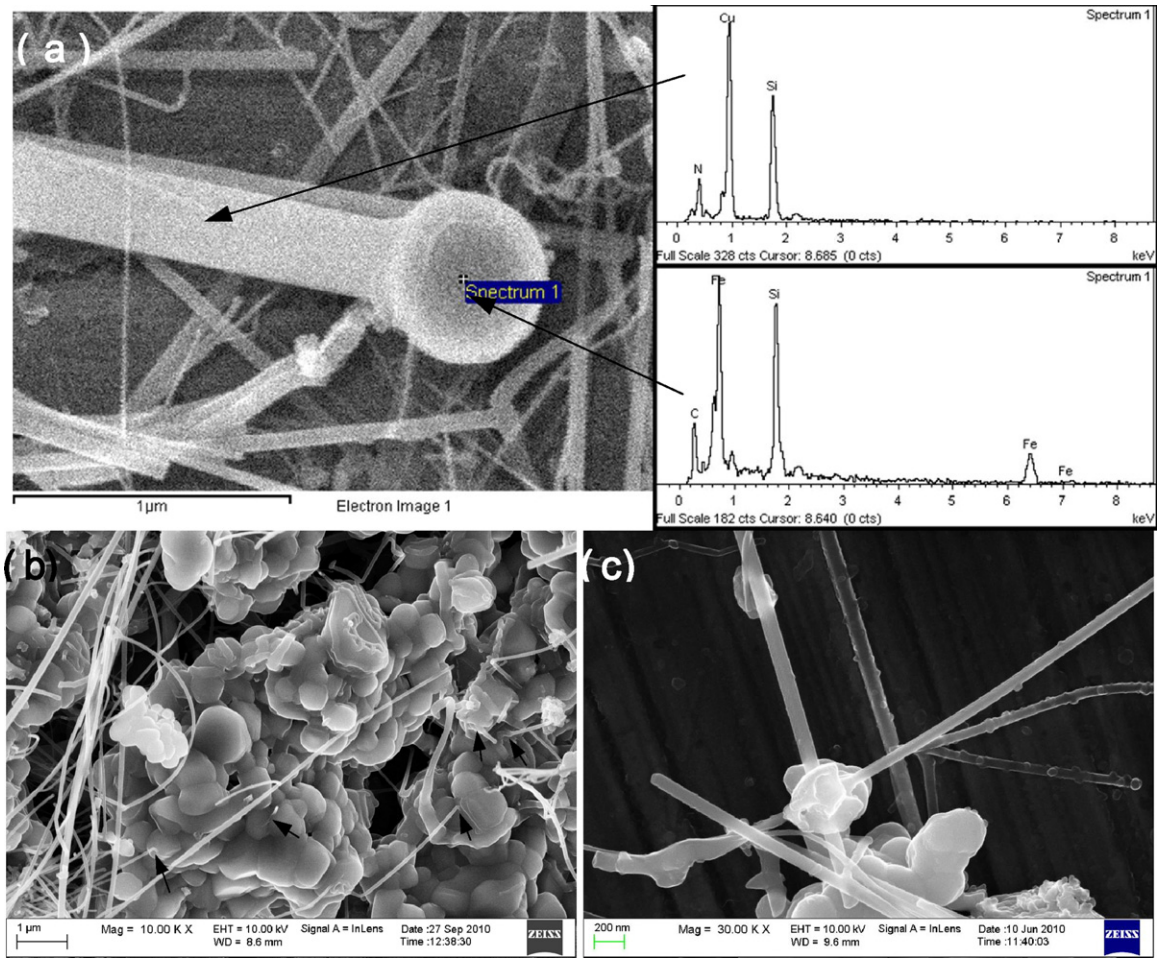

Fig. 7. (a) FESEM image of one nanowire with a droplet and corresponding nanochemical data: EDS (top) of the nanowire, and EDS (bottom) of the droplet. (b) FESEM image showing the roots of nanowires (labeled with black arrow). (c) FESEM image showing that a nanowire grew from the interspace among several particles.

Besides, Si atoms were limited in the vapour phase at the experimental condition, so most nanowires grew via SLGS mechanism instead of VLS mechanism. The comparatively wide range of the nanowire diameters could be ascribed to abrupt fluctuations in experimental temperature which can influence the size of Si_3N_4 crystal nucleus. Several reasons exist to explain why only Si_3N_4 (and not SiC) nanowires were formed. Firstly, Si_3N_4 is thermodynamically more stable than SiC in the experimental condition, namely below 1400 °C and under 2 MPa N_2 [30]. Secondly, Yang et al. [36] reported that the stoichiometry of the iron silicide is a key parameter for precipitation of SiC. If the Fe content is high (e.g. Fe_3Si), carbon will be precipitated instead of SiC. The XRD pattern (Fig. 3) indicates that, during combustion process, the catalyst of Fe worked in the form of Fe_3Si, which was unfavorable to the precipitation of SiC from the liquid alloy. Lastly, it is well known that iron promotes the dissociation of N_2, thus the presence of iron facilitated the formation of Si_3N_4 in the liquid alloy [14,37]. The relationship between growth mechanisms and growth directions of Si_3N_4 nanowires needs a further study.

Besides, PTFE additives played an important role in the CS of the composite powders. Firstly, it can promote the reaction of silicon and carbon. It is well known that the reaction of silicon and carbon is a weak exothermic reaction ($\Delta H = -16.6$ kcal/mol) and the released heat can not ensure a self-propagating mode of the reaction. In combustion synthesis, silicon carbide can be synthesized via using the heat of other highly exothermic reactions. In our study, two highly exothermic reactions were used to activate the weak exothermic reaction of silicon and carbon. One is the nitridation of silicon ($\Delta H = -198.15$ kcal/mol) which has been mentioned previously, and the other is the following reaction [22]:

$$\mathrm{Si(s)} + (-\mathrm{C_2F_4}-)_n\mathrm{(s)} \rightarrow \mathrm{SiF_4(g)} + \mathrm{C(s)}.$$

Secondly, after decomposition, PTFE can provide a sufficient space for the growth of Si_3N_4-NWs. Lastly, PTFE can also promote the growth of Si_3N_4-NWs by creating higher temperature gradient.

Summarily, the combined thermal effects of highly and weak exothermic reactions provided a moderate temperature between 1200 °C and the melting point of Si (1412 °C), which is widely used for the fabrication of α-Si_3N_4 nanowires [13–15,17–19]. During the combustion process, SiC particles were formed by the reaction of silicon and carbon in a nonequilibrium process and the iron powders catalyzed the in situ formation of Si_3N_4-NWs by VLS and SLGS mechanisms.

4. Conclusions

In summary, large-scale composite powders containing SiC particles and Si_3N_4-NWs were prepared by cost effective combustion synthesis, using the mixture of Si, carbon black, PTFE and a small amount of iron powders as the precursor. The SiC particles are equiaxed with diameters in the micron range. The Si_3N_4-NWs are straight with uniform diameters of 20–350 nm and lengths of tens of microns. The growth directions of the nanowires were characterized to be [1 0 1] and [1 0 0]. VLS and SLGS processes are proposed as the growth mechanisms of the nanowires, and the SLGS mechanism played a main role. We believe the as-synthesized composite powders have great potential in the fabrication of high-performance SiC/Si_3N_4-NW composites. Further studies of their applications on ceramics are in progress.

Acknowledgement

This work was supported by Chinese National Fusion Project for ITER (No. 2010GB109000).

References

[1] Y. Fu, Y.W. Gu, H. Du, SiC whisker toughened Al_2O_3-(Ti, W) C ceramic matrix composites, Scripta Mater. 44 (1) (2001) 111–116.
[2] G.Y. Lin, T.C. Lei, S.X. Wang, Y. Zhou, Microstructure and mechanical properties of SiC whisker reinforced ZrO_2 (2 mol% Y_2O_3) based composites, Ceram. Int. 22 (3) (1996) 199–205.
[3] G.Y. Lin, T.C. Lei, Microstructure, mechanical properties and thermal shock behaviour of Al_2O_3 + ZrO_2 + SiCw composites, Ceram. Int. 24 (4) (1998) 313–326.
[4] P.F. Becher, G.C. Wei, Toughening behavior in SiC-whisker-reinforced alumina, J. Am. Ceram. Soc. 67 (12) (1984) C-267–C-269.
[5] Y. Hua, L. Zhang, L. Cheng, J. Wang, Silicon carbide whisker reinforced silicon carbide composites by chemical vapor infiltration, Mater. Sci. Eng. A 428 (1–2) (2006) 346–350.
[6] A.E. Giannakopoulos, K. Breder, Synergism of toughening mechanisms in whisker-reinforced ceramic-matrix composites, J. Am. Ceram. Soc. 74 (1) (1991) 194–202.
[7] C.R. Jones, C.H. Henager Jr., R.H. Jones, Crack bridging by SiC fibers during slow crack growth and the resultant fracture toughness of SiC/SiC_f composites, Scripta Metall. Mater. 33 (12) (1995) 2067–2072.
[8] W. Yang, A. Kohyama, T. Noda, Y. Katoh, T. Hinoki, H. Araki, et al., Interfacial characterization of CVI-SiC/SiC composites, J. Nucl. Mater. 307–311 (part 2) (2002) 1088–1092.
[9] E.W. Wong, P.E. Sheehan, C.M. Lieber, Nanobeam mechanics: elasticity, strength, and toughness of nanorods and nanotubes, Science 277 (5334) (1997) 1971–1975.
[10] Z. Xia, L. Riester, W.A. Curtin, H. Li, B.W. Sheldon, J. Liang, et al., Direct observation of toughening mechanisms in carbon nanotube ceramic matrix composites, Acta Mater. 52 (4) (2004) 931–944.
[11] W. Yang, H. Araki, C. Tang, S. Thaveethavorn, A. Kohyama, H. Suzuki, et al., Single-crystal SiC nanowires with a thin carbon coating for stronger and tougher ceramic composites, Adv. Mater. 17 (12) (2005) 1519–1523.
[12] W. Yang, H. Araki, A. Kohyama, S. Thaveethavorn, H. Suzuki, T. Noda, Process and mechanical properties of in situ silicon carbide-nanowire-reinforced chemical vapor infiltrated silicon carbide/silicon carbide composite, J. Am. Ceram. Soc. 87 (9) (2004) 1720–1725.
[13] H. Cui, B.R. Stoner, Nucleation and growth of silicon nitride nanoneedles using microwave plasma heating, J. Mater. Res. 16 (11) (2001) 3111–3115.
[14] F. Wang, G.Q. Jin, X.Y. Guo, Formation mechanism of Si_3N_4 nanowires via carbothermal reduction of carbonaceous silica xerogels, J. Phys. Chem. B 110 (30) (2006) 14546–14549.
[15] F. Wang, G.Q. Jin, X.Y. Guo, Sol–gel synthesis of Si_3N_4 nanowires and nanotubes, Mater. Lett. 60 (3) (2006) 330–333.
[16] X.C. Wu, W.H. Song, W.D. Huang, M.H. Pu, B. Zhao, Y.P. Sun, et al., Simultaneous growth of α-Si_3N_4 and β-SiC nanorods, Mater. Res. Bull. 36 (5-6) (2001) 847–852.
[17] G. Shen, Y. Bando, B. Liu, C. Tang, Q. Huang, D. Golberg, Systematic investigation of the formation of 1D α-Si_3N_4 nanostructures by using a thermal-decomposition/nitridation process, Chem. Eur. J. 12 (11) (2006) 2987–2993.
[18] F. Chen, Y. Li, W. Liu, Q. Shen, L. Zhang, Q. Jiang, et al., Synthesis of α silicon nitride single-crystalline nanowires by nitriding cryomilled nanocrystalline silicon powder, Scripta Mater. 60 (9) (2009) 737–740.
[19] W. Han, S. Fan, Q. Li, B. Gu, Synthesis of silicon nitride nanorods using carbon nanotube as a template, Appl. Phys. Lett. 71 (16) (1997) 2771–2773.
[20] C.C. Chen, C.L. Li, K.Y. Liao, A cost-effective process for large-scale production of submicron SiC by combustion synthesis, Mater. Chem. Phys. 73 (2–3) (2002) 198–205.
[21] O. Yamada, K. Hirao, M. Koizumi, Y. Miyamoto, Combustion synthesis of silicon carbide in nitrogen atmosphere, J. Am. Ceram. Soc. 72 (9) (1989) 1735–1738.
[22] K. Yang, Y. Yang, Z.M. Lin, J.T. Li, J.S. Du, Mechanical-activation-assisted combustion synthesis of SiC powders with polytetrafluoroethylene as promoter, Mater. Res. Bull. 42 (9) (2007) 1625–1632.
[23] Z. Yermekova, Z. Mansurov, A. Mukasyan, Influence of precursor morphology on the microstructure of silicon carbide nanopowder produced by combustion syntheses, Ceram. Int. 36 (8) (2010) 2297–2305.
[24] H.B. Jin, M.S. Cao, Y.X. Chen, J.T. Li, S. Agathopoulos, The influence of mechanochemical activation on combustion synthesis of Si_3N_4, Ceram. Int. 34 (5) (2008) 1267–1271.
[25] Y. Yang, Y.X. Chen, Z.M. Lin, J.T. Li, Synthesis of α-Si_3N_4 using low-α-phase Si_3N_4 diluent by the seeding technique, Scripta Mater. 56 (5) (2007) 401–404.
[26] Y. Chen, Z. Lin, J. Li, J. Du, S. Yang, PTFE an effective additive on the combustion synthesis of silicon nitride, J. Eur. Ceram. Soc. 28 (1) (2008) 289–293.
[27] M.A. Rodriguez, N.S. Makhonin, J.A. Escriña, I.P. Borovinskaya, M.I. Osendi, M.F. Barba, et al., Single crystal β-Si_3N_4 fibers obtained by self-propagating high temperature synthesis, Adv. Mater. 7 (8) (1995) 745–747.
[28] Y.G. Cao, H. Chen, J.T. Li, C.C. Ge, S.Y. Tang, J.X. Tang, et al., Formation of α-Si_3N_4 whiskers with addition of NaN_3 as catalyst, J. Cryst. Growth 234 (1) (2002) 9–11.
[29] J.P. Nicolich, Z. Lences, W. Dressler, R. Riedel, Phase quantification of β-Si_3N_4/β-SiC mixtures by X-ray powder diffraction analysis, J. Mater. Sci. 35 (6) (2000) 1427–1432.
[30] H.J. Seifert, J. Peng, H.L. Lukas, F. Aldinger, Phase equilibria and thermal analysis of Si–C–N ceramics, J. Alloys Compd. 320 (2) (2001) 251–261.
[31] R.S. Wagner, W.C. Ellis, Vapor–liquid–solid mechanism of single crystal growth, Appl. Phys. Lett. 4 (5) (1964) 89–90.
[32] R.Q. Zhang, Y. Lifshitz, S.T. Lee, Oxide-assisted growth of semiconducting nanowires, Adv. Mater. 15 (7-8) (2003) 635–640.
[33] T.J. Trentler, K.M. Hickman, S.C. Goel, A.M. Viano, P.C. Gibbons, W.E. Buhro, Solution–liquid–solid growth of crystalline III–V semiconductors: an analogy to vapor–liquid–solid growth, Science 270 (5243) (1995) 1791–1794.
[34] W. Yang, L. Zhang, Z. Xie, J. Li, H. Miao, L. An, Growth and optical properties of ultra-long single-crystalline α-Si_3N_4 nanobelts, Appl. Phys. A: Mater. Sci. Process. 80 (7) (2005) 1419–1423.
[35] W. Yang, Z. Xie, J. Li, H. Miao, L. Zhang, L. An, Ultra-long single-crystalline α-Si_3N_4 nanowires: derived from a polymeric precursor, J. Am. Ceram. Soc. 88 (6) (2005) 1647–1650.
[36] G. Yang, R. Wu, M. Gao, J. Chen, Y. Pan, SiC crystal growth from transition metal silicide fluxes, Cryst. Res. Technol. 42 (5) (2007) 445–450.
[37] H.M. Jennings, Review on reactions between silicon and nitrogen, part 1: mechanisms, J. Mater. Sci. 18 (4) (1983) 951–967.